

2002

# Development Of A Piston-Cylinder Expansion Device For The Transcritical Carbon Dioxide Cycle

J. S. Baek  
*Purdue University*

E. A. Groll  
*Purdue University*

P. B. Lawless  
*Purdue University*

Follow this and additional works at: <http://docs.lib.purdue.edu/iracc>

---

Baek, J. S.; Groll, E. A.; and Lawless, P. B., "Development Of A Piston-Cylinder Expansion Device For The Transcritical Carbon Dioxide Cycle" (2002). *International Refrigeration and Air Conditioning Conference*. Paper 584.  
<http://docs.lib.purdue.edu/iracc/584>

This document has been made available through Purdue e-Pubs, a service of the Purdue University Libraries. Please contact [epubs@purdue.edu](mailto:epubs@purdue.edu) for additional information.

Complete proceedings may be acquired in print and on CD-ROM directly from the Ray W. Herrick Laboratories at <https://engineering.purdue.edu/Herrick/Events/orderlit.html>

**DEVELOPMENT OF A PISTON-CYLINDER EXPANSION DEVICE  
FOR THE TRANSCRITICAL CARBON DIOXIDE CYCLE**

J.S. Baek, E.A. Groll and P.B. Lawless

Purdue University  
Ray W. Herrick Laboratories  
West Lafayette, IN 47907, USA

**ABSTRACT**

Carbon dioxide is receiving strong consideration as an alternative refrigerant substituting hydrochlorofluorocarbons (HCFCs) and chlorofluorocarbons (CFCs) due to its zero ozone depletion potential and negligible global warming potential. The system performance of CO<sub>2</sub> systems, however, is typically poor compared to the current conventional air conditioning systems using HCFC or CFC. One of the most effective ways to achieve parity with CFC and HCFC systems is to replace the expansion valve with an expansion device that minimizes entropy creation and allows for energy recovery during the expansion process.

A piston-cylinder type work output expansion device was designed, constructed and tested as part of the study reported here. The device is based on a highly modified small four-cycle, two-piston engine with a displacement of 2 x 13.26 cm<sup>3</sup> that is commercially available. The work out expansion device replaced the expansion valve in an experimental transcritical CO<sub>2</sub> cycle and increased the system performance by up to 10%.

**INTRODUCTION**

Chlorofluorocarbons (CFCs) and hydrochlorofluorocarbons (HCFCs) will be phased out as refrigerants due to their potential to destroy the ozone layer of the earth's atmosphere. Although hydrofluorocarbons (HFCs) have zero ozone depletion potential, they have a significant global warming potential and their future use has been questioned as well. Therefore, substances with no ozone depletion potential and no or negligible global warming potential, e.g., natural fluids such as carbon dioxide, ammonia, hydrocarbons, and water, are being considered as alternative refrigerants. Carbon dioxide (CO<sub>2</sub>) is nontoxic and non-flammable, has zero ozone depletion potential, and negligible global warming potential as a refrigerant. It thus is close to being the ideal refrigerant except that its thermodynamic cycle characteristics result in system COPs that are typically lower than HFC vapor compression systems.

Figure 1 shows the schematic of the typical transcritical CO<sub>2</sub> cycle and Figure 2 illustrates the cycle on a temperature-entropy (T-s) diagram. As shown in Figure 1, the basic transcritical CO<sub>2</sub> cycle consists of a compressor, a gas cooler, an expansion valve and an evaporator. The cycle is composed of four basic processes; compression (1-2), heat rejection (2-3), expansion (3-4h) and heat absorption (4-1) as shown in Figure 2. In the expansion process, the paths 3-4s and 3-4h represent isentropic expansion and isenthalpic expansion, respectively. In the compression process, the paths 1-2s and 1-2 stand for the isentropic and actual processes, respectively.

Carbon dioxide is receiving strong consideration for automobile and military applications due to its high volumetric heat capacity, and the elimination of recovery and recycling equipment and the subsequent procedures. Because of its high volumetric heat capacity, CO<sub>2</sub> offers the potential for reduced weight and volume in packaged systems, which is a major focus for transportable field units in the military. For example, the U.S. Army is seeking an air conditioning system with significant weight and size reduction and higher efficiency, resulting in reducing tactical power generator sizes [Patil, 1998].

The performance of a carbon dioxide based air conditioning system may be less than that of HFC or HCFC based air conditioning systems due to the thermodynamic characteristics of the transcritical cycle. Robinson and Groll compared the Coefficient Of Performances (COPs) of a packaged air conditioner using HCFC-22 as the refrigerant with the ones of a carbon dioxide based packaged air conditioner by using computer simulation models [Robinson and Groll, 2000]. Their analysis showed that for a packaged air conditioner application using the same

evaporator size and capacity, the transcritical CO<sub>2</sub> air conditioner will operate with a COP, which is similar to the simulated performance of an U.S. Army packaged air conditioner, which uses HCFC-22 as the refrigerant.

Robinson conducted a parametric study which compared the actual performance of a HFC-134a based automobile air conditioner and the performance of a carbon dioxide based automobile air conditioner [Robinson, 2000]. His analysis system showed that for an automobile application, the prototype transcritical CO<sub>2</sub> cycle device introduced by Pettersen will operate with a COP which is 66-75% (average 70%) of the experimentally determined COP of a production HFC-134a based automobile air conditioner while providing the same evaporator capacity.

System improvements, therefore, need to be achieved to meet the goal of the reduction of weight and volume while still maintaining the same or higher system efficiency. One way to increase the system performance among several methods is to replace the expansion valve with an expansion device. As the carbon dioxide expands through the device, not only is energy recovered but also the enthalpy at the inlet to the evaporator becomes smaller resulting in an increase in evaporator capacity. This process is shown in Figure 2 (the process of 3-4w). As shown in this figure, the entropy generation will decrease with the expansion device.

### **PISTON-CYLINDER EXPANSION DEVICE**

A piston-cylinder type system was selected to design and construct a work output expansion device. The piston-cylinder expansion device consists of a cylinder, piston and connecting rod as shown in Figure 3. The piston is connected to a crank mechanism that drives the shaft. The shaft in turn is connected to a mechanical loading device to absorb the extracted energy. The expansion process is controlled using fast-acting solenoid valves as intake and exhaust valves. The expansion device is referred to as ED-WOW, which stands for Expansion Device With Output Work.

There are three processes that must occur within the time period of one revolution: intake, expansion and exhaust. During the intake process, the intake valve opens and the supercritical high pressure CO<sub>2</sub> flows into the cylinder and pushes the piston down from Top Dead Center (TDC) to the Location Of Expansion initiation (LOE) as shown in Figure 3. When the piston reaches LOE, the intake valve closes and the expansion process begins with the piston moving down further, as the CO<sub>2</sub> expands from high pressure and temperature to low pressure and temperature. When the piston reaches Bottom Dead Center (BDC), the exhaust valve opens. During the second stroke the expanded CO<sub>2</sub> is swept out to the inlet of the evaporator as the piston moves up. When the piston again reaches TDC, the exhaust valve closes, the intake valve opens, and the next cycle begins. Figure 4 shows the ideal expansion processes in a p-v diagram.

The ED-WOW replaces the expansion valve in the transcritical CO<sub>2</sub> cycle as shown in the schematic in Figure 5. The enthalpy of carbon dioxide at the outlet of the expansion device becomes less than at the outlet of the expansion valve. Therefore, the heat removal capacity of the evaporator increases through the use of a work output expansion device. In addition, if the work that is generated during the expansion is used to assist the compression work, the system performance can be significantly increased. Table 1 shows the operating condition of the transcritical CO<sub>2</sub> cycle that provided the basis for the design of the ED-WOW.

### **Design of Cylinder, Piston, and Crank of Expansion Device**

The prototype piston-cylinder work output expansion device is based on a highly modified four-cycle, two-piston engine with a displacement of  $2 \times 13.26 \text{ cm}^3$  that is commercially available. In the original design, both pistons were in the same firing order, meaning that both pistons achieve TDC at the same time. In the CO<sub>2</sub> expander application, the goal is to reduce the need for mechanical inertia (e.g., a flywheel) by using an out-of-phase firing order, with the piston on the expansion stroke providing the force required to drive the opposing piston through the exhaust stroke. Therefore, the piston, piston ring, and connecting rod of the commercially available engine were assembled with a modified crankshaft that provides out-of-phase firing order in the original engine housing.

### **Design of Control Valves**

The expansion process is designed to be controlled using fast-acting solenoid valves as intake and exhaust valves. As there will be some time lag for the solenoid valves to response to an input signal, the flow characteristics of the valve have to be determined. Towards this end, experiments were performed to characterize the filling behavior of CO<sub>2</sub> into the ED-WOW. For this purpose, a fixed-volume chamber was designed that represents the volume of the ED-WOW at the instant of time on the expansion stroke when the intake valve is required to close. In

order to guarantee minimum throttling in the expansion device, the time that takes for the CO<sub>2</sub> to fill the chamber volume and to pressurize the chamber up to the pressure upstream of the intake valve needs to be known. Figure 6 shows the schematic of the experimental setup.

A fast acting solenoid valve with 3/64-inch orifice diameter was tested. A dynamic pressure transducer was installed in the chamber to characterize the filling process in the test chamber after energizing the solenoid valve. This transducer is AC coupled, and thus only provides the unsteady portion of the pressure signal. Therefore, the peak of the unsteady signal indicates when the volume can be considered 'filled'. Figures 7 and 8 show the pressure signal (in Volts) as CO<sub>2</sub> fills the chamber. In the legend of the figures,  $p_1$  and  $p_2$  stand for the initial pressures upstream of the valve and in the chamber, respectively. As shown in these figures, the pressure starts to increase approximately 0.01 seconds after opening of the valve, this period being the physical lag time between the initiation of the control signal and the motion of the valve.

It can be seen from Figure 7 that the time that it takes to reach the maximum pressure increases slightly as the inlet pressure increases. Figure 8 shows the comparison of the pressure increase for similar absolute pressure differences across the solenoid valve, but with different inlet pressures. From Figure 8 it can be seen that the time that it takes to reach the maximum pressure decreases as the inlet pressure increases. As shown in Figures 7 and 8, it takes more than 0.075 seconds for the pressures to reach maximum values. The design calculation shows that the possible valve opening time is approximately 0.072 seconds. Therefore, it was determined that two intake valves and one exhaust valve must be used in order to provide a large enough flow area into the piston-cylinder chamber for the design application.

Additional experiments were conducted without CO<sub>2</sub> flow, i.e., no pressure difference across the valve to measure the valve closing time. The average response time to the signal to close the solenoid valve with 3/64-inch orifice diameter is 0.05323 s and its 95% confidence interval is 0.05253-0.05393 s. This time is taken as the representative time required to close the intake and exhaust valves.

### **Example of Valve Control**

Figure 9 shows the desired piston displacement from the top ceiling of the piston-cylinder device over time as determined from the ED-WOW design. The assumed revolutionary speed is 120 rpm and the lengths of the connecting rod and crank are 38.8 mm and 11.0 mm. Also indicated in this figure are the timings for the intake and exhaust valves. The analysis indicates that the intake valve should open at the TDC at time zero and close when the piston reaches 5.21 mm from TDC (at the displacement of 8.01 mm) at 0.072 seconds. The exhaust valve should open at the displacement of 24.80 mm (Bottom Dead Center, BDC) at 0.25 seconds and close when the piston reaches the TDC again. The timings for the control signals required for the valves to fully open and fully close are indicated in the figure. The circle and square in Figure 9 stand for the timings of input signal to open and close the intake and exhaust valves, respectively.

### **Design of Cylinder Head**

The cylinder head connects the dual intake and single exhaust solenoid valves to the cylinder. The major design constraint for the device was achieving the absolute minimum dead volume in the system (i.e. the volume downstream of the intake valve at piston top dead center). This minimal dead volume is critical to achieving an efficient expansion process, as it is directly proportional to throttling losses at the beginning of the expansion stroke. Figure 10 presents several views of the cylinder head design, showing the three ports that allow for connection of the valves. Each of the two cylinder heads is bolted to the crankcase with four machine screws. The three valves for each head connect via 1/8 in. NPT fittings, and in turn are attached to a retention plate (not shown) with machine screws. Tie rods span between the cylinder head retention plates on each of the two opposed cylinders, allowing for a rigid structure resistant to vibration-induced leakage in the head gasket. Figure 11 shows the assembly of the piston-cylinder chamber, the top of the expander header, and the solenoid valves.

### **Design of Enclosure**

The prototype ED-WOW was designed to operate at an inlet pressure of 1500 psig and an outlet pressure of 500 psig. Due to these high pressures, it was anticipated that some CO<sub>2</sub> will leak from the expansion volume to the crank housing along the piston rings, and from the crank housing to the surrounding environment through bearings and seals. Therefore, the whole ED-WOW was placed in an enclosure to prevent the refrigerant from leaking out of the system. The enclosure is under discharge pressure as it is intended that the CO<sub>2</sub> exiting the discharge valve

enters the enclosure. Thus, the enclosure needs to be strong enough to withstand the discharge pressure of about 500 psig during normal operation. Figure 12 shows the design of the enclosure including ED-WOW.

## EXPERIMENTS

The expansion device, referred to as ED-WOW (Expansion Device –With Output of Work), was installed in a prototype transcritical CO<sub>2</sub> cycle. Figure 13 shows the transcritical CO<sub>2</sub> cycle with the ED-WOW. As shown in the figure, a conventional expansion valve is located in parallel to the ED-WOW. This valve is used as a bypass line that fraction of the CO<sub>2</sub> mass flow rate that could not be accepted by the ED-WOW.

A mechanical loading device is connected to the ED-WOW to absorb the energy extracted from CO<sub>2</sub> during the expansion process. A hydraulic pump is used as the loading device. Figure 14 shows the schematic of the connection of the ED-WOW and the loading device. As shown in Figure 14, static pressures are measured before and after the pump, and the volumetric flow rate of the water (the working fluid) is measured using a rotameter. The ideal pump work is then calculated using the pressure difference across the pump and the water flow rate as follows:

$$P_{HP} = \Delta p \cdot \dot{V} \quad (1)$$

Where,  $P_{HP}$ ,  $\Delta p$ , and  $\dot{V}$  stand for the pump power, pressure difference across the hydraulic pump, and water volumetric flow rate. The work produced through the ED-WOW is measured indirectly using the hydraulic pump power and its efficiency as follows:

$$P_{ED-WOW} = \frac{P_{HP}}{\epsilon_{HP}} \quad (2)$$

Where,  $\epsilon_{HP}$  and  $P_{ED-WOW}$  represent hydraulic pump efficiency and work produced through the ED-WOW, respectively.

### Experimental Test Conditions

Experiments were performed at three different operating conditions. Table 3 shows the experimental conditions for each case. The indoor temperature,  $T_{indoor}$ , and outdoor temperature,  $T_{outdoor}$ , were 20°C and 35°C, respectively.  $P_{c,out}$ ,  $P_{c,in}$ ,  $T_{c,out}$ , and  $T_{c,in}$  indicate the compressor discharge pressure, compressor suction pressure, compressor discharge temperature, and compressor suction temperature, respectively. The compressor discharge pressure ranged from 6621 kPa to 7971 kPa and the compressor suction pressure varied from 2528 kPa to 2771 kPa. The compressor discharge temperatures ranged from 88°C to 118°C and the compressor suction temperature was approximately 20°C for all cases.  $\dot{m}_{CO_2}$  represents the CO<sub>2</sub> mass flow rate in the system and the values of 9.7 kg/s to 13.5 g/s were determined based on the compressor capacity.  $\omega_{ED}$  and  $\Delta t_{intake}$  are the rotational speed and the intake valve opening time of the ED-WOW.

$P_{gc,in}$ ,  $P_{gc,out}$ ,  $P_{ED,in}$ ,  $P_{ED,out}$ , and  $p_{evap,out}$  are the pressures at the inlet and outlet of the gas cooler, at the inlet and outlet of the ED-WOW, and at the outlet of the evaporator, respectively.  $T_{gc,in}$ ,  $T_{gc,out}$ ,  $T_{ED,in}$ , and  $T_{evap,out}$  are the temperature at the inlet and outlet of the gas cooler, at the inlet of the ED-WOW, and at the outlet of the evaporator, respectively.

### Cycle Performance

Figure 15 shows the p-h diagram of the processes of the system for three experiments. The numbers in the figure indicate the state points. The same state points are also shown in Figure 13. As shown in Table 3 and Figure 15, the pressure at the outlet of the compressor of 7971 kPa, is higher than the critical pressure of CO<sub>2</sub> (7377 kPa, [ASHRAE, 1997]) only in Case 3.

There is a relatively large pressure drop from state 4, outlet of the gas cooler, to state 5, at the inlet of the ED-WOW. This is due to the many valves and fittings and the internal heat exchanger (IHX) between these states as shown in Figures 13 and 14. These valves have been arranged to measure the mass flow rate of CO<sub>2</sub> during the experiment. It can also be seen in the figure that the pressure decreases from the outlet of the evaporator to the inlet of the compressor. This is caused by the internal heat exchanger and the accumulator between the evaporator and compressor.

The process from state 5 to state 7 stands for the case of the isenthalpic expansion process (assuming an expansion through an ordinary expansion valve) in Figure 15. As expected, the enthalpy decreases at the inlet of the evaporator when CO<sub>2</sub> expands through the ED-WOW even though the amount of the enthalpy decrease does not seem great.

As previously mentioned, the work generated through the ED-WOW has been measured indirectly by measuring the power of the hydraulic pump. The efficiency of the pump was measured at approximately 50% at an ED-WOW speed of 300 RPM. As the design speed of the ED-WOW in the current tests is 120 RPM, the pump efficiency can be expected to be less than this value. As the actual pump efficiency could not be measured at this low rpm, the pump efficiency was assumed to be 50% which will thus provide a conservative estimate of the work extracted from the ED-WOW.

The measured works produced by the ED-WOW are 23.2 W, 28.7 W, and 34.8 W for Cases 1, 2, and 3, respectively as shown in Table 4. As the pressure difference across the ED-WOW increases, the work produced increases as well. The measured isentropic efficiency of the ED-WOW ( $\epsilon_{s,ED}$ ) is about 10%. Table 4 and Table 5 show the results of the experiments.  $P_{ED,in}$ ,  $P_{ED,out}$ , and  $T_{ED,in}$  stand for the pressures at the inlet and outlet of the ED-WOW and temperature at the inlet of the ED-WOW, respectively.  $\dot{Q}_{isenth}$  and  $\dot{Q}_{ED}$  represent the evaporator capacity when CO<sub>2</sub> expands through the ordinary expansion valve and the ED-WOW, respectively. As discussed above, the evaporator capacity increases with the CO<sub>2</sub> expansion through the ED-WOW.  $\dot{W}_{comp}$  and  $\dot{W}_{ED}$  illustrate the compressor work and the work produced through the ED-WOW, respectively.  $COP_{EXV}$  is the COP based on the isenthalpic expansion.  $COP_{ED-1}$  and  $COP_{ED-2}$  are the COPs based on utilizing the ED-WOW.  $COP_{ED-1}$  is the COP of the system when only the “lower-enthalpy-effect” is considered.  $COP_{ED-2}$  is the COP when in addition to the “lower-enthalpy-effect” the work output of the ED-WOW is used to reduce the compressor work input. The COPs are calculated as follows:

$$COP_{EXV} = \frac{\dot{Q}_{isenth}}{\dot{W}_{comp}} \quad (3)$$

$$COP_{ED-1} = \frac{\dot{Q}_{ED}}{\dot{W}_{comp}} \quad (4)$$

$$COP_{ED-2} = \frac{\dot{Q}_{ED}}{\dot{W}_{comp} - \dot{W}_{ED}} \quad (5)$$

It can be seen from Tables 4 and 5 that the COP increases through the use of the ED-WOW. If only the lower-enthalpy-effect is considered, the COP increases by 3.3% to 5.4% compared to the COP based on the isenthalpic expansion. If both, the lower-enthalpy-effect and compressor work reduction are considered, the COP increased by 6.7% to 9.9%. As mentioned previously, the hydraulic pump efficiency that is used to calculate the work output of the ED-WOW is a conservative estimate. If a more accurate efficiency at the given condition is used, it is likely that the work output through the ED-WOW will be larger than the value resulting in a greater improvement in the system performance.

As shown in Table 4, the capacity of the evaporator increases with an increase of the high side pressure (compressor discharge pressure). In addition, the work produced through the ED-WOW increased as  $P_{c,out}$  increases. However, the percentage of the increase of the evaporator and  $COP_{ED-1}$  decreases with the increase of the  $P_{c,out}$ . The largest percentage for the increase of  $\dot{Q}_{ED}$  and  $COP_{ED-1}$  occurs in Case 1. If both, lower-enthalpy-effect and work output effects are considered, there is the tendency that the system performance improvement decreases with an increase in  $P_{c,out}$ . The largest improvement of the system performance occurs in Case 1 (lowest compressor discharge pressure, 6621 kPa) and it is 9.9%. When the compressor discharge pressure is the highest (7971 kPa, Case 3), the system efficiency improvement becomes the smallest at 6.7% even though the absolute amounts of enthalpy decrease at the inlet of the evaporator and work output through the ED-WOW are the largest.

## CONCLUSIONS

A prototype piston-cylinder work output expansion device was designed, constructed and tested. The design was based on a highly modified small four-cycle, two-piston engine of displacement  $2 \times 13.26 \text{ cm}^3$  that is commercially available. Fast-acting solenoid valves were used as intake and exhaust valves to control the expansion process. Due to the time lag between the input signal and the opening and closing of the solenoid valves, the revolution speed of the crankshaft was set to 120 RPM.

The work output expansion device replaced the expansion valve in an experimental transcritical  $\text{CO}_2$  cycle. The expansion device minimizes the entropy creation and recovers energy during the expansion process. The use of the work output expansion device increased the system performance by up to 10%.

## REFERENCES

1. ASHRAE, 1997, "ASHRAE fundamentals handbook", American Society of Heating, Refrigerating and Air-Conditioning Engineers, Inc., 1997 edition.
2. Ashok S. Patil, 1998, "Natural working fluids – Military advantages and opportunities", *IIR – Gustav Lorentzen Conference, Joint Meeting of the International Institute of Refrigeration*, Section B and E, Oslo, Norway.
3. Douglas M. Robinson, 2000, "Modeling of carbon dioxide based air-to-air air conditioners", Ph.D. Thesis, Purdue University.
4. D. M. Robinson and E. A. Groll, 2000, "Theoretical performance comparison of  $\text{CO}_2$  transcritical cycle technology versus HCFC-22 technology for a military packaged air conditioner application", *International Journal of Heating, Ventilating, Air-Conditioning and Refrigeration Research*, Vol. 6, No. 4: pp. 325-348.

## ACKNOWLEDGEMENTS

The study presented in this paper is funded by the United States Air Force. The authors would like to thank the U.S. Air Force for the sponsorship.

Table 1: Specifications of the transcritical  $\text{CO}_2$  cycle to which the work output expansion device was applied.

Parameter	Value	Unit
Mass flow	0.04	kg/s
High side pressure	10.2	MPa
Low side pressure	3.4	MPa
Gas cooler outlet temperature	322.2	K

Table 2: Relevant engine parameters.

Parameters used by Jeng, and Radakovic and Khonsari	Values	Unit
Engine speed	$S = 2000$	rpm
Cylinder bore	$B = 88.9$	mm
Bore radius	$r = 44.45$	mm
Crank radius	$R = 40.0$	mm
Connecting rod length	$L = 141.9$	mm
Composite roughness	$\sigma = 0.5$	$\mu\text{m}$
Piston ring width	$b = 1.475$	mm
Ring thickness	$t_r = 3.8$	mm
Ring modulus	$E = 70.0$	$\text{GN/m}^2$
Ring crown height	$C_R = 14.9$	$\mu\text{m}$
Friction coefficient	$f = 0.08$	-
Lubricant viscosity	$\mu = 0.00689$	$\text{Pa} \cdot \text{s}$
Tangential ring tension	$T = 22.38$	N

Table 3: Test conditions to investigate the performance of the ED-WOW.

Case	1	2	3
$T_{\text{indoor}}$ (°C)	20	20	20
$T_{\text{outdoor}}$ (°C)	35	35	35
$P_{\text{c,out}}$ (kPa)	6620.7	7068.7	7971.3
$P_{\text{c,in}}$ (kPa)	2770.9	2637.3	2528.2
$P_{\text{gc,in}}$ (kPa)	6603.5	7045.3	7938.2
$P_{\text{gc,out}}$ (kPa)	6536.9	6931.5	7845.2
$P_{\text{ED,in}}$ (kPa)	6052.1	6392.4	7255.7
$P_{\text{ED,out}}$ (kPa)	2921.7	2814.3	2759.8
$P_{\text{evap,out}}$ (kPa)	2854.8	2735.7	2657.4
$T_{\text{c,out}}$ (°C)	87.6	99.4	117.9
$T_{\text{c,in}}$ (°C)	20.2	19.8	19.6
$T_{\text{gc,in}}$ (°C)	68.0	77.6	93.7
$T_{\text{gc,out}}$ (°C)	36.0	36.2	36.7
$T_{\text{ED,in}}$ (°C)	26.0	27.9	31.4
$T_{\text{evap,out}}$ (°C)	12.5	11.0	10.3
$\dot{m}_{\text{CO}_2}$ (g/s)	9.7	11.6	13.5
$\omega_{\text{ED}}$ (RPM)	114	120	120
$\Delta t_{\text{intake}}$ (s)	0.129	0.123	0.123

Table 4: Results of the experiments with ED-WOW in a transcritical CO<sub>2</sub> cycle.

Case	1	2	3
$P_{\text{ED,in}}$ (kPa)	6052.1	6392.4	7255.7
$P_{\text{ED,out}}$ (kPa)	2921.7	2814.3	2759.8
$T_{\text{ED,in}}$ (°C)	26.0	27.9	31.4
$\dot{Q}_{\text{isenth}}$ (W)	425.6	570.7	1030
$\dot{Q}_{\text{ED}}$ (W)	448.7	599.4	1064
$\dot{W}_{\text{comp}}$ (W)	567.6	773.1	1110
$\dot{W}_{\text{ED}}$ (W)	23.18	28.70	34.77
$\text{COP}_{\text{EXV}}$	0.7498	0.7382	0.9279
$\text{COP}_{\text{ED-1}}$	0.7905	0.7753	0.9586
$\text{COP}_{\text{ED-2}}$	0.8242	0.8052	0.9896
$\epsilon_{\text{s,ED}}$	10.47	9.97	10.27

Table 5: Increase of the evaporator capacity and COP.

Case	1	2	3
$\dot{Q}_{\text{isenth}}$ (W)	425.6	570.7	1030
$\dot{Q}_{\text{ED}}$ (W)	448.7	599.4	1064
Increase of evaporator capacity (%)	5.43	5.03	3.30
$\text{COP}_{\text{EXV}}$	0.7498	0.7382	0.9277
$\text{COP}_{\text{ED-1}}$	0.7905	0.7753	0.9586
Increase of COP with enthalpy effect only (%)	5.43	5.03	3.30
$\text{COP}_{\text{ED-2}}$	0.8242	0.8052	0.9896
Increase of COP with enthalpy & work output effects (%)	9.92	9.08	6.67

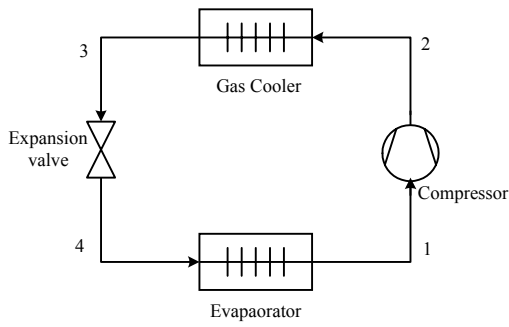


Figure 1: Schematic of basic transcritical carbon dioxide cycle.

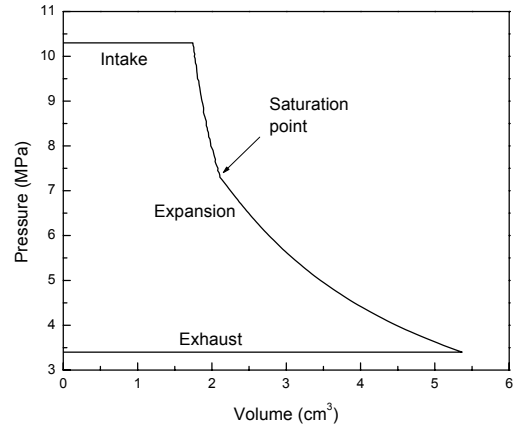


Figure 4: Piston processes with assumption of ideal process.

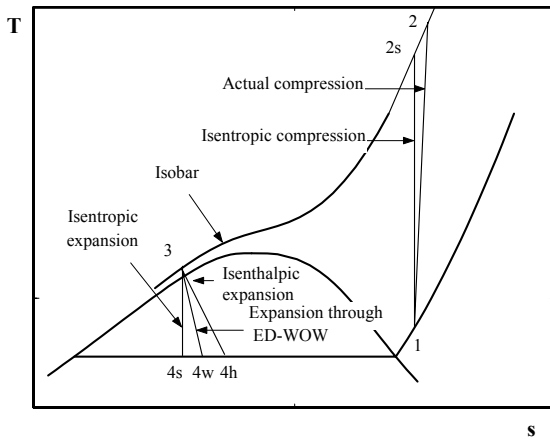


Figure 2: Temperature-entropy diagram of transcritical carbon dioxide cycle.

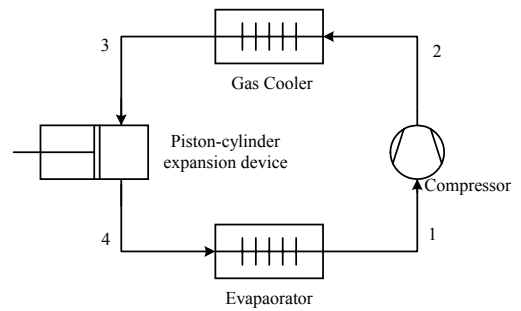


Figure 5: Schematic of transcritical CO<sub>2</sub> cycle with piston-cylinder expansion device replacing expansion valve.

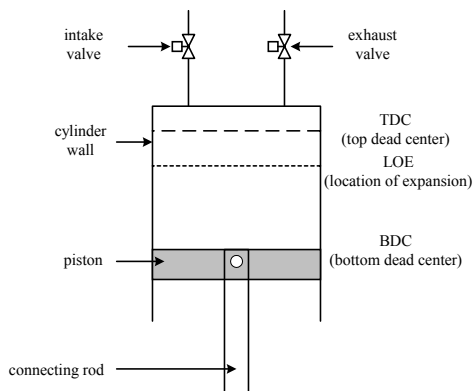


Figure 3: Piston-cylinder device with the related components and piston positions.

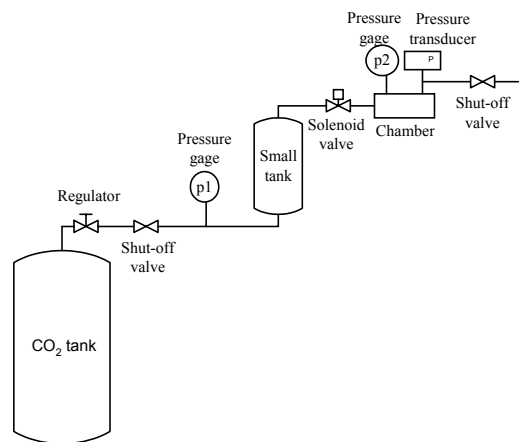


Figure 6: Schematic of test stand to determine the opening time of the intake valve.

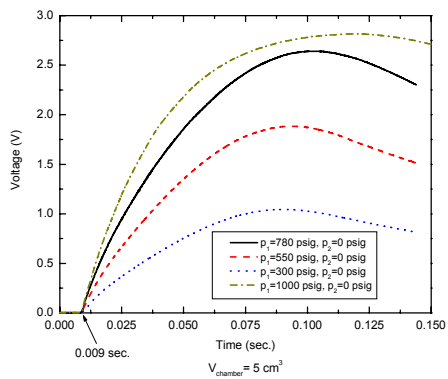


Figure 7: Filling behaviors of CO<sub>2</sub> in the chamber with the intake valve ( $D_{\text{orifice}}=3/64$  in).

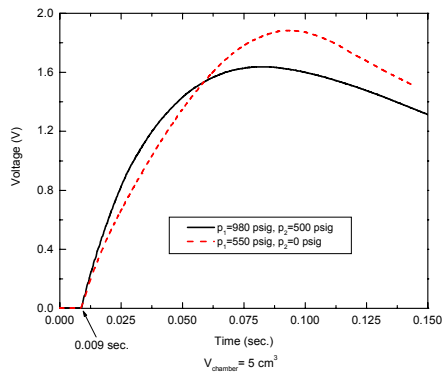


Figure 8: Comparison of filling behaviors for similar pressure differences, but with different  $p_1$ s.

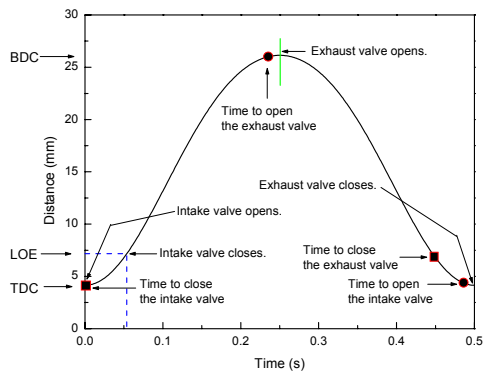


Figure 9: Timings for input signals to the solenoid valves.

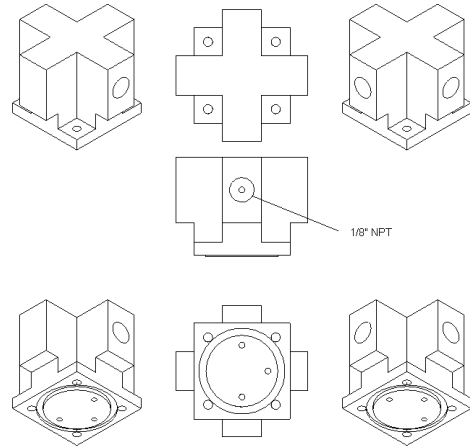


Figure 10: Several views of the head of the piston-cylinder device.

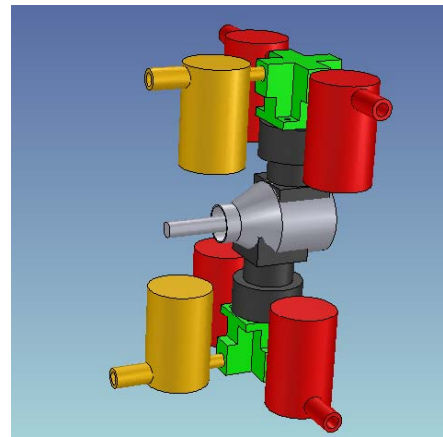


Figure 11: Assembly of Piston-cylinder work extraction expansion device.

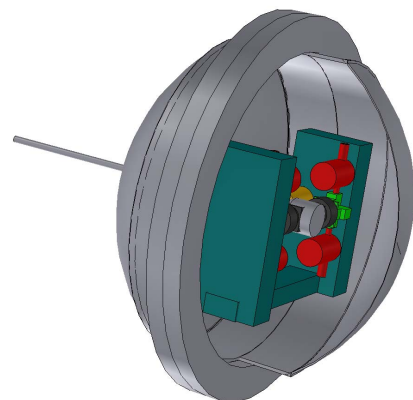


Figure 12: Cut view of the designed enclosure with expansion device in scale.

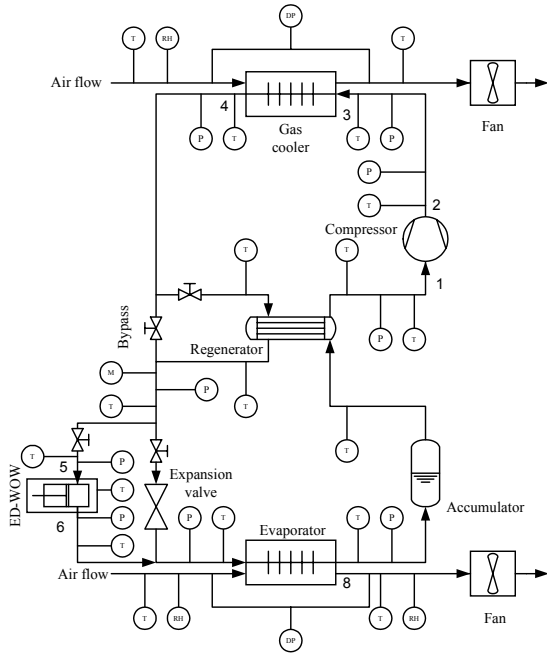


Figure 13: Experimental setup of transcritical CO<sub>2</sub> cycle with ED-WOW

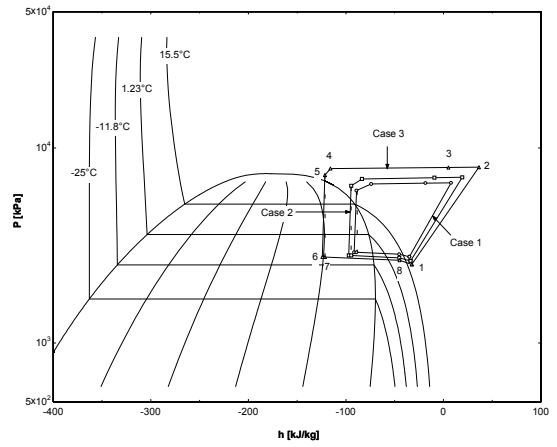


Figure 15: Pressure-enthalpy diagram of the system processes.

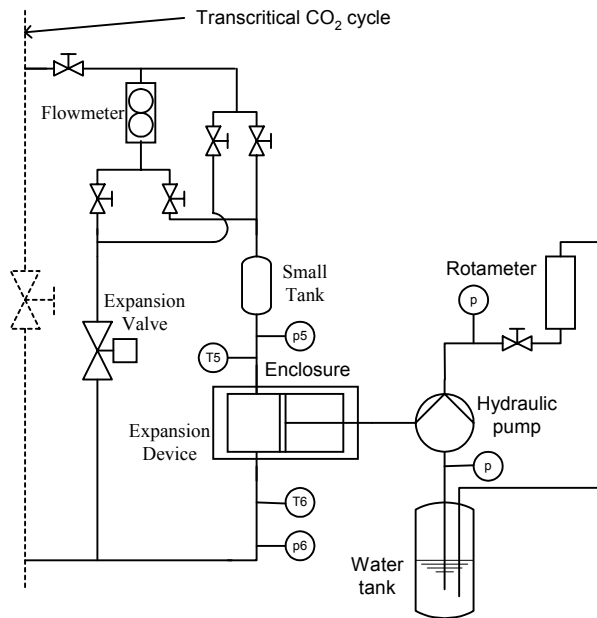


Figure 14: Connection of the ED-WOW to the mechanical loading device.